EXPERIMENTAL STUDY OF IMPURITY INTERACTION EFFECTS IN AgPd

By K. Królas

Institute of Physics, Jagellonian University, Cracow*

B. Wodniecka and P. Wodniecki

Institute of Nuclear Physics, Cracow**

(Received April 21, 1980)

The perturbed γ-γ angular correlation technique is applied to studies of the interaction of impurity atoms in silver. The effect of attraction between In and Pd impurities leading to the creation of the nearest neighbour impurity pairs in the silver lattice is found. The results are discussed within the frame of two different models which consider the electronic or elastic interaction between two impurity atoms in a metal.

PACS numbers: 61.70.Wp

1. Introduction

The interaction between impurity atoms in a dilute alloy system is an interesting problem in metal physics. The nature of this problem is rather complex and its understanding is based on the electronic structure or on the elastic interaction of the impurities in a metal. In the electronic approach the excess or deficiency of impurity charge is screened by the conduction electrons and creates an oscillating electric potential which leads to attraction or repulsion of other impurity atoms [1]. In the elasticity approach [2] the interaction is correlated with impurity volumes and can also be attractive or repulsive depending on impurity sizes and location among the lattice atoms.

Both approaches, the elasticity and electronic one, are clearly related and show two aspects of the same problem. However, a unified description of the interaction does not exist. Just as little precise experimental information is available on the exact structure of impurity-impurity interactions in various metallic systems.

In the present work the interaction between In and Pd impurities in silver is studied.

* Address: Instytut Fizyki UJ, Reymonta 4, 30-059 Kraków, Poland.
** Address: Instytut Fizyki Jądrowej, Radzikowskiego 152, 31-342 Kraków, Poland.

Silver and palladium form a continuous series of solid solutions in a broad range of temperatures and for all relative concentrations [3]. Thus, the Pd impurities are randomly distributed around any Ag atom in a dilute silver alloy. However, if another impurity atom such as In is introduced into the system, it is not at all obvious that the Pd distribution around that particular atom will be still random. In fact, one expects that both the size and charge screening effects will lead to attraction or repulsion of the Pd impurities by the In atom.

The impurity situation can be characterized by its electric quadrupole interaction with surrounding atoms. In a pure metal with cubic structure the electric field gradient (EFG) at each lattice site vanishes due to the charge symmetry. An impurity atom generally destroys this symmetry and induces an EFG at the neighbouring lattice sites. When a radioactive probe is introduced in the impurity neighbourhood this EFG can be measured with the time differential perturbed angular correlation (TDPAC) technique, as was done in the present work.

The magnitude of the EFG at the probing nucleus depends on the distance from the impurity atom to the probe and in the case when more than one impurity atom is present in the neighbourhood of the probe, it depends on the impurity atom distribution over the neighbouring lattice sites. When all lattice sites are equally favoured for the impurity location, many various impurity-probe configurations in the lattice occur and the probe nuclei are exposed to EFG's of various magnitudes. However, it was shown recently that for some cases a surprisingly large fraction of probes in silver dilute alloys is exposed to the same EFG's magnitude [4–6]. It was explained assuming a non-random impurity distribution around the probe atoms caused by an impurity interaction. The energy of this interaction can be determined.

In the present work, the hyperfine quadrupole interaction of ^{111}Cd in AgPd alloys was investigated for the ^{111}Cd isotope populated either from the ^{111}Ag or from the ^{111}In decay. It was found that after ^{111}Ag decay the ^{111}Cd probes in AgPd alloys were surrounded by Pd impurities distributed in a statistical way, the same as for other host silver atoms. After ^{111}In decay, however, the ^{111}Cd probe environment was found to be nonstatistically occupied by Pd impurities due to an In-Pd interaction in silver. It was concluded that this interaction leads to the creation of In-Pd pairs in neighbouring substitutional sites of the silver lattice.

2. Experimental procedure

Two types of $Ag_{1-x}Pd_x$ samples containing either ^{111}Ag or ^{111}In activity were prepared in the following way. In order to obtain the $Ag_{0.97}Pd_{0.03}(^{111}Ag)$ sample, 5 mg of natural palladium were irradiated with thermal neutrons for 4 days with a neutron flux of 10^{13}n/cm^{2}s. Three days after the irradiation most of the ^{111}Pd, which had been produced by the neutron capture of ^{110}Pd, decayed yielding the wanted ^{111}Ag activity. A proper amount of pure silver was then added to the irradiated palladium to get the $Ag_{0.97}Pd_{0.03}(^{111}Ag)$ alloy.

To obtain $Ag_{1-x}Pd_x(^{111}In)$ samples (x ranging from 0.0003 to 0.03) a 50 μm thick silver foil was irradiated with 27 MeV α-particles. The irradiation lasted 8 hours with an

average beam intensity of 3 μA. 36 hours after the irradiation the ^{111}In activity arose via ^{109}Ag(α, 2n)^{111}In reaction was practically the only activity left in the target. A suitable piece of the silver target, containing about 10 μCi of ^{111}In activity, was then melted under an argon atmosphere with palladium in order to obtain the wanted $Ag_{1-x}Pd_x(^{111}In)$ alloy. After melting, all $Ag_{1-x}Pd_x(^{111}In)$ samples as well the $Ag_{0.97}Pd_{0.03}(^{111}Ag)$ one were annealed for 2 hours at 900 K. The concentration of ^{111}Ag and ^{111}In probes in the samples was ca 10^{-3} ppm while the concentration of all alien impurities in the alloys was estimated, assuming the purity of the silver and palladium, to be less than 10 ppm.

The standard fast-slow coincidence set-up with three NaJ(T1) detectors was used to record simultaneously two coincidence time spectra $N(\theta, t)$ for the angle θ, between the detectors, equal to 180° and 90°. Here, t denotes the delay time between the emission of

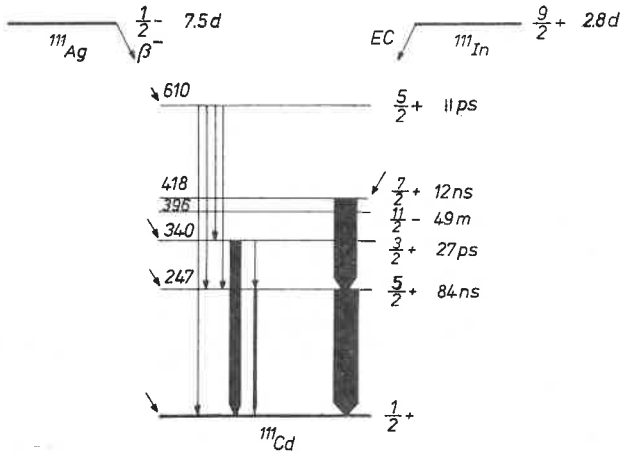

Fit. 1. The decay scheme of ^{111}Ag and ^{111}In isotopes

the first and second γ ray. The start detector observed the 95 keV or 174 keV γ rays for the decays of ^{111}Ag or ^{111}In, respectively, while two stop detectors observed the 247 keV radiation for both angular correlation measurements (see Fig. 1).

Two runs of the angular correlation measurements with ^{111}Cd fed in ^{111}Ag decay were performed in $Ag_{0.97}Pd_{0.03}$, each lasting about 3 weeks. The measurements of the angular correlation after ^{111}In decay were performed for five AgPd alloys differing in palladium concentration and lasted 1–2 days for each alloy.

3. *Analysis and results*

The observed time coincidence spectra exhibit the exponential decay modulated by the time-dependent angular correlation function $W(\theta, t)$.

$$N(\theta, t) = N_0 e^{-t/\tau} W(\theta, t), \tag{1}$$

where τ is the lifetime of the 247 keV intermediate state. For the case of random orientations of EFG's the angular correlation function for the two gamma cascades considered here is theoretically [7] of the form

$$W(\theta, t) = 1 + A_2 G_2(t) P_2(\cos\theta), \tag{2}$$

where A_2 denotes the angular correlation coefficient characteristic for a given gamma cascade. The perturbation factor $G_2(t)$ contains information on the EFG acting on the probe nucleus. The quantity $A_2G_2(t)$ can be simply extracted from the experimentally obtained time-dependent counting rate

$$R(t) = 2 \cdot \frac{N(180°, t) - N(90°, t)}{N(180°, t) + 2N(90°, t)} = A_2 G_2(t). \tag{3}$$

The $A_2G_2(t)$ spectra derived from angular correlation measurements are shown in Figs. 2 and 3.

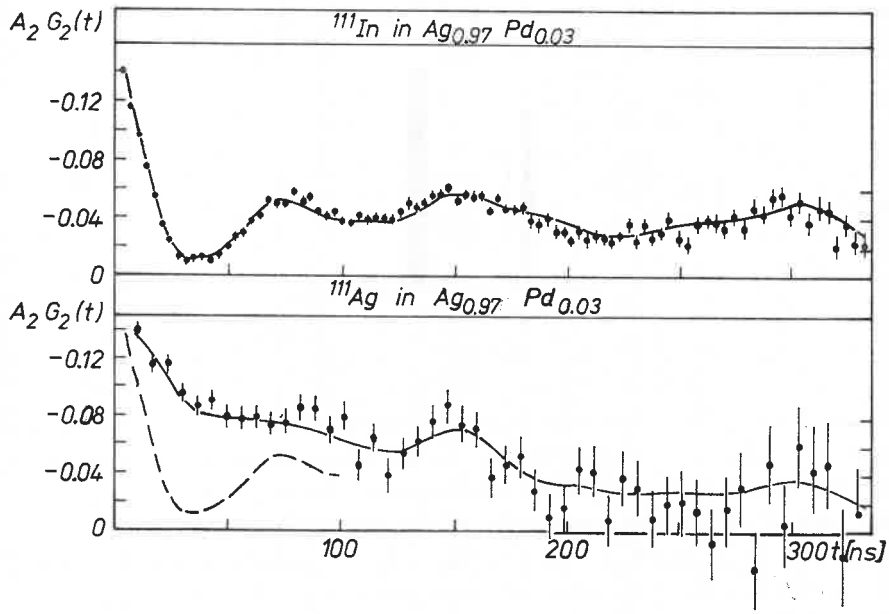

Fig. 2. TDPAC spectra of ^{111}Cd after decays of ^{111}Ag and ^{111}In in $Ag_{0.97}Pd_{0.03}$. Solid lines are the fits of Eqs. (7) and (6) for ^{111}In and ^{111}Ag experiments, respectively. Dash curve is drawn to compare the results of both experiments

The EFG is fully given by the two parameters: its z-component V_{zz} and the asymmetry parameter $\eta = (V_{xx} - V_{yy})/V_{zz}$. Here, V_{xx}, V_{yy} and V_{zz} are the components of the EFG tensor at the probing nucleus in the principial axis system chosen in such a way that $|V_{xx}| \leqslant |V_{yy}| \leqslant |V_{zz}|$. For details see Ref. [8].

The perturbation factor of the angular correlation for a static quadrupole interaction and for the spin 5/2 of the intermediate state can be expressed by [7]

$$G_2(t) = \sum_{n=1}^{3} s_{2n}(\eta) \cos \omega_n(\eta) t, \tag{4}$$

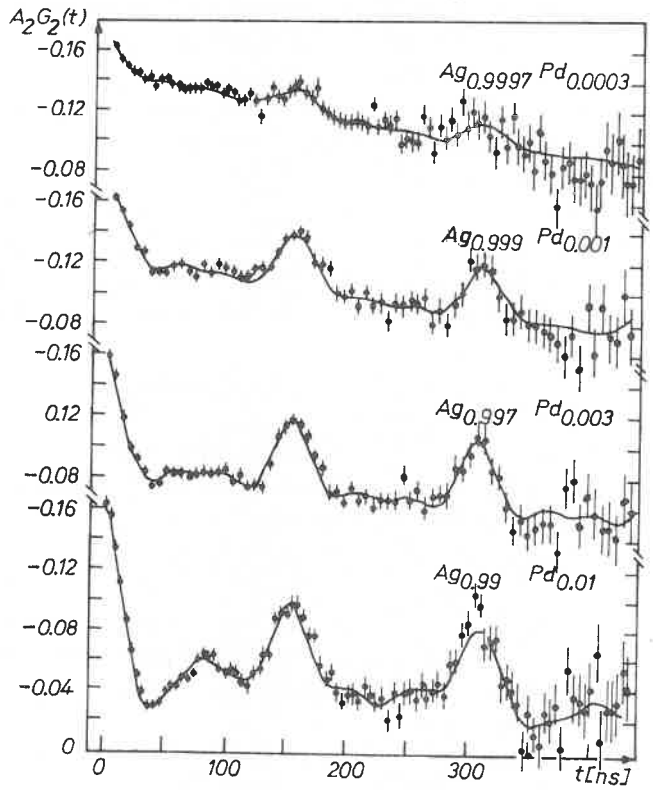

Fig. 3. TDPAC spectra of ^{111}Cd in $Ag_{1-x}Pd_x$(^{111}In) alloys. Solid curves are the results of the least squares fits of Eq. (7)

where $s_{2n}(\eta)$ are tabulated coefficients and $\omega_n(\eta)$ are the transition frequencies depending on V_{zz} and η. For $\eta = 0$ the ω_n are: $\omega_1 = \frac{10}{3\pi} \nu_Q$, $\omega_2 = 2\omega_1$, and $\omega_3 = 3\omega_1$. The quadrupole coupling constant ν_Q is given by

$$\nu_Q = \frac{eQV_{zz}}{h}, \tag{5}$$

where eQ is the quadrupole moment of the probe nucleus which for ^{111}Cd in the 247 keV excited state equals 0.77 ± 0.12b [9]. When the different probe nuclei are exposed to the EFG's of different magnitudes the $G_2(t)$ depends on the distribution of the V_{zz} and η.

The resulting $G_2(t)$ can be written as

$$G_2(t) = \frac{1}{m} \sum_{k=1}^{m} G_2^k(t), \tag{6}$$

where summing runs over all m probe nuclei and $G_2^k(t)$ is the perturbation factor expressed by (4) with V_{zz}^k and η^k describing the EFG acting on the k-probe nucleus. In cubic alloys different probe atoms are placed in sites of different distances from impurities and therefore are exposed to the EFG's of different magnitudes.

To smiplify an analysis of the results of the EFG measurements in cubic alloys some information on the impurity distribution among the lattice sites is necessary. No short range order in AgPd alloys was observed [3]. Therefore, the random distribution of Pd atoms around all host silver atoms including ^{111}Ag probes in $Ag_{0.97}Pd_{0.03}(^{111}Ag)$ can be assumed. On the other hand in the case of ^{111}In probes this assumption turns out not to be valid and one has to take into account only a few specific probe-impurity configurations. Therefore, two different approaches to the data analysis were used for the ^{111}Ag and ^{111}In probes.

The time dependent ratio $R(t)$ obtained for ^{111}Ag in $Ag_{0.97}Pd_{0.03}$ alloys were analysed using the following assumptions:

a) all lattice sites are equally favoured for the impurity atom location

b) one impurity atom produces at the neighbouring lattice site an axially symmetric EFG with the z axis coinciding with the impurity-probe direction

c) the EFG produced by more than one impurity is a sum of the EFG tensors corresponding to each impurity.

The components V_{zz}^i of the EFG's produced by a single impurity atom occupying a lattice site on the i-th shell around the probe were taken as free parameters. In the calculations only the four nearest shells were taken into account.

The Monte Carlo method was employed to generate the random impurity distribution around one lattice site, chosen as the ^{111}Ag probe site. Next, the EFG corresponding to this impurity distribution was determined by summing the contributions of all impurities occupying sites within a sphere of a radius equal to the fourth nearest neighbour distance. Then the EFG tensor was diagonalized and its components were expressed by the V_{zz}^i. This procedure was repeated 10^3 times and finally the resulting $G_2(t)$ was found as a sum of $m = 10^3$ components $G_2^k(t)$ for the EFG determined for each impurity distribution. The resulting $G_2(t)$ being a function of four V_{zz}^i parameters was fitted to the $R(t)$ obtained in the experiment.

The observed spectra for ^{111}In in AgPd alloys shown in Fig. 3 look differently from those obtained in the ^{111}Ag case. These spectra exhibit a well-defined quadrupole interaction characteristic to a specific probe-impurity configuration in the sample. Therefore, results of these measurements were fitted only with two, and for alloys with impurity concentration $x \geqslant 0.003$ with three different contributions c_i corresponding to different probe-impurity configurations:

$$R(t) = A_2 G_2(t) = A_2[c_1 G_2^1(t) + c_2 G_2^2(t) + c_3 G_2^3(t)]. \tag{7}$$

In the first step of analysis $G_2^1(t)$, $G_2^2(t)$ and $G_2^3(t)$ were the perturbation factors expressed by (4). The following results were obtained. The c_1 fraction of ^{111}Cd interacts with an axially symmetric EFG with $V_{zz} = V_{zz}^1$ independent of the impurity concentration. The c_2 fraction of probes is exposed to an EFG with V_{zz}^2 component 1.25 times larger than V_{zz}^1. The $c_3 = 1-c_1-c_2$ fraction of ^{111}Cd experiences a very weak EFG with $V_{zz}^3 \approx 0$. The good fits were obtained when each EFG was assumed not unique, but described by a Lorentzian V_{zz} distribution with a width σ [5]. To reduce the number of free parameters in the next step of analysis the following parameters were kept constant: $\eta_1 = 0$, $\eta_3 = 0$, $V_{zz}^2 = 1.25\, V_{zz}^1$ and $V_{zz}^3 = 0$. The results of the least squares fits of the function (7) to the experimental points are shown in Fig. 3 and the fitted parameters are listed in Table II.

4. Discussion

The observed resultant EFG at the probe atoms in dilute alloys reflects, firstly the occupation of the lattice shells around the probe by impurity atoms and secondly, the contributions to EFG produced by impurities in the different shells around the probe. Information about the shell occupation and the EFG from an impurity in a certain shell cannot be easily deduced separately.

With the use of two different parent activities as probe atoms a different occupation of lattice sites by impurities around probe atoms can be achieved, if the binding energy between impurity and probe atoms are considerably different. Since the two parent activities decay to the same daughter nuclei, the observation of the same EFG for both parent activities points directly to a specific impurity-probe situation.

TABLE I

Quadrupole interaction results for a Pd impurity situated on the first, second, third and fourth (i = 1, 2, 3 and 4) shell at a distance r_i from the ^{111}Cd probe in the silver lattice

Number of shell i	1	2	3	4
V_{zz}^i [10^{17} Vcm^{-2}][a]	2.31 (0.09)	0.95 (0.21)	0.19 (0.18)	0.24 (0.11)
ν_Q^i [MHz]	43.0 (1.7)	17.7 (4.0)	3.5 (3.3)	4.4 (2.0)
$\nu_Q^i (r^i)^3$ [arbitrary units]	1	1.17 (0.23)	0.42 (0.40)	0.82 (0.35)

[a] The eQ error is not included.

Assuming that the shell occupation in $Ag_{0.97}Pd_{0.03}$(^{111}Ag) is simply given by a random distribution of Pd atoms, the quadrupole coupling constant for the ^{111}Cd-Pd nearest neighbour configuration equal to 43.0 ∓ 1.7 MHz was found (see Table I). This value is in full agreement with the quadrupole coupling constant for a large fraction of ^{111}Cd populated in ^{111}In decay in $Ag_{1-x}Pd_x$(^{111}In) alloys (see Table II).

This agreement strongly supports the conclusion that the well-defined quadrupole interaction occurring in the ^{111}In spectra arises from the nearest neighbour probe-impurity

configuration. Because the fraction of the probe nuclei exposed to this nearest neighbour EFG is much higher than it would be for a random impurity distribution, an attractive In-Pd interaction in silver is suggested. This interaction leads to the creation of InPd atom pairs in the substitutional nearest neighbour lattice sites of silver. The quadrupole coupling

TABLE II

Least squares fit parameters for ^{111}In in $Ag_{1-x}Pd_x$ alloys. The c_1 and c_2 are fractions of the probes exposed to the two different EFG described by ν_Q^1 and $\eta_1 = 0$ and $\nu_Q^2 = 1.25\,\nu_Q^1$ and η_2, respectively

x	c_1	c_2	ν_Q^1 [MHz]	η_2
0.0003	0.09 (2)	—	42.8 (7)	—
0.001	0.24 (2)	—	43.1 (8)	—
0.003	0.33 (4)	0.10 (3)	43.4 (4)	0.66 (5)
0.01	0.40 (3)	0.33 (4)	44.6 (7)	0.61 (3)
0.03	0.26 (2)	0.61 (4)	44.4 (5)	0.63 (2)

constant 43.0 MHz corresponds to $V_{zz} = 2.3 \cdot 10^{17}$ V cm^{-2} of the EFG produced on the Cd probe by the nearest neighbour Pd atom in the silver lattice.

In principle, the quantitative analysis of the EFG produced by the distributed charges requires an understanding of the EFG sources in metallic systems. In general terms it is a very difficult task and usually simple models are used.

In the simplest approach of the point charge model, the EFG from an impurity should vary as r^{-3}. This dependence can be compared with the experimentally obtained V_{zz}^i at ^{111}Cd after the ^{111}Ag decay. The data were fitted with four values of V_{zz}^i as free parameters attributed to the four nearest shells around ^{111}Cd. The observed weights correspond to the coordination numbers of the first four shells which are 12, 6, 24 and 12 for a fcc lattice. Unfortunately, except for V_{zz}^1, all other V_{zz}^i values have rather large experimental errors, but they are consistent with the r^{-3} dependence of the point charge model (see Table I). Similar behaviour of the EFG for different probe-impurity distances was observed in aluminium rich alloys [10].

The point charge model can be also employed to describe the probe-impurity configuration which leads to the nonaxial EFG acting on the probes in $Ag_{1-x}Pd_x(^{111}In)$ alloys with $x \geqslant 0.003$. Simple calculations of the EFG due to two impurity atoms being the nearest neighbours to the probe, show that in 8 among 11 possible positions in the fcc lattice, the EFG is nonaxional with the asymmetry parameter $\eta = 0.6$ and its z-component is 1.25 times larger than the V_{zz} due to one impurity. The results presented in Table II show that the c_2 fraction of the ^{111}Cd probes after ^{111}In decay in $Ag_{1-x}Pd_x$ is exposed to the EFG with asymmetry parameter $\eta_2 \approx 0.6$ and V_{zz} component 1.25 times larger than V_{zz}^1. Hence it is reasonable to assume that the c_2 fraction of the probes has two impurities in the nearest neighbourhood. The c_2 value is also much higher than it would be for a random impurity distribution. This indicates that the attraction of the Pd impurity by In is not saturated by one Pd atom, but a second Pd atom is attracted as well in order to form an $InPd_2$ complex.

Further support for the conclusion of the creation of the impurity complexes in silver comes from the c_1 and c_2 dependence on Pd impurity concentration. For very dilute alloys ($x < 0.003$) the case of only one Pd atom trapping was observed. As can be seen in Fig. 4, a number of In probes having one Pd nearest neighbour rises with impurity concentration

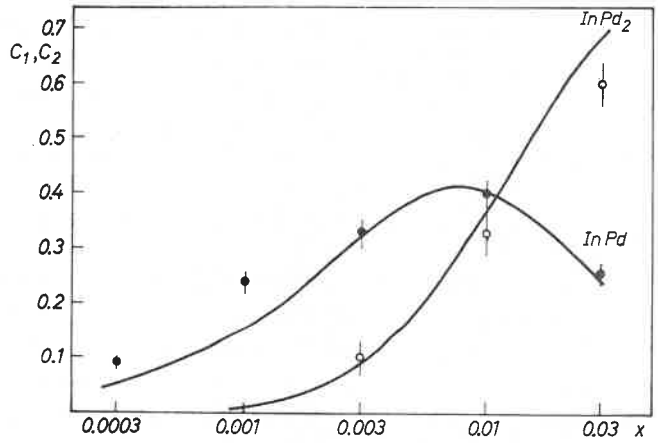

Fig. 4. The c_1 (solid points) and c_2 (open circles) dependences on the palladium impurity concentration x. The curves denote the dependences of the number of the InPd and $InPd_2$ impurity complexes on x derived from the mass action low (see text)

up to $x = 0.01$. A decrease of the InPd pair number for $x = 0.03$ can be understood by taking into account the rise in the number of $InPd_2$ complexes observed for $x \geqslant 0.003$.

The solid curves in Fig. 4 were drawn assuming that the concentrations of InPd and $InPd_2$ complexes are given by the mass action law [11]. The binding energies were taken to be the same for both reaction constants k_1 and k_2 but the preexponential entropy term for k_2 is twice as high as for k_1 because of the number of possible impurity atom configurations.

Knowing that for In and Pd impurities the nearest neighbour configuration is energetically favoured, one can attempt to explain the binding energy within the electronic and the elasticity approach.

Blandin and Deplante [1], discussing the potential produced by the impurity charge excess screened by the conduction electrons, found that in monovalent metals such as silver this potential leads to an attractive interaction between two impurities of opposite charge differences. For In and Pd in silver, the valency differences of the impurities and the host atoms can be assumed to be $Z_1(\mathrm{In}) = +2$ and $Z_2(\mathrm{Pd}) = -1$. The binding energy E_B concluded from the asymptotic form of the electron screening potential

$$V(r) = \frac{Z_1}{k_F(2k_F+1)^2} \frac{\cos 2k_F r}{r^3},$$

where k_F is the Fermi wave vector, is estimated as

$$E_B = -Z_1 Z_2 \cdot 0.03 \text{ eV}.$$

Hence, the interaction between In and Pd in silver is predicted to be attractive with $E_B = 60$ meV, while the binding energy calculated from the exact form of the screening potential was obtained to be 115 meV. This value is in reasonable agreement with the experimental value 135 ± 9 meV for In-Pd complexes [5], which were identified here as the nearest neighbour impurity pairs.

In the elasticity model for impurity interactions in metals Eshelby found [2] that for impurity atoms, the sizes of which differ from the host atom size, there are directions in the fcc lattice for which the interaction is attractive. Because the lattice constant of the AgPd alloy decreases with palladium concentration, $\frac{da}{dc} = -2.5 \cdot 10^{-3}$ Å/at % and the lattice constant of the AgIn alloy increases with indium concentration, $\frac{da}{dc} = +3.3 \cdot 10^{-3}$ Å/at % [12] one can consider Pd and In impurities in silver as undersized and oversized atoms, respectively. In this case the model of the elastic impurity interaction in fcc metals predicts an attraction in the ⟨100⟩ direction. The interaction energy for the ⟨110⟩ direction never has the maximum value for any impurity size. Results of our measurements, however, which show that the InPd impurity pairs are formed in the ⟨110⟩ direction are in disagreement with the prediction of the elastic impurity interaction model of Eshelby.

The creation of three impurity atom complexes e.g. $InPd_2$, was not discussed in the frame of the mentioned models. But basing on the electronic model the attraction of the second Pd atom by an InPd pair can be intuitively understood assuming that the indium charge excess $+2$ is not saturated by the -1 charge excess of the first trapped Pd impurity and the net charge of the InPd pair still leads to the attraction of the next Pd impurity.

In conclusion, the model of electronic interaction between impurities in metals can qualitatively explain the experimental finding of the attraction between In and Pd impurities in silver. This model, however, gives only a rough agreement between measured and calculated binding energies. This is not surprising because the electronic model does not take into account the energy of the lattice distortion in the impurity neighbourhood. A detailed calculation and further experimental investigation are necessary to find the exact description of the nature of the impurity interaction in metallic systems.

We would like to thank Professors G. Schatz, A. Z. Hrynkiewicz and H. Bernas for helpful and valuable comments on a preliminary draft of this paper.

REFERENCES

[1] A. Blandin, J. L. Deplante, *Metallic Solid Solutions*, Eds. J. Friedel and A. Guinier, Benjamin, New York 1963, IV.
[2] J. D. Eshelby, *Acta Metall.* **3**, 487 (1955).
[3] K. M. Myles, *Acta Metall.* **13**, 109 (1965).
[4] R. Butt, H. Haas, H. Rinneberg, *Phys. Lett.* **60A**, 323 (1977).
[5] K. Królas, B. Wodniecka, P. Wodniecki, *Hyperfine Interactions* **4**, 605 (1978).
[6] J. A. H. Da Jornada, I. J. R. Baumvol, M. Behar, R. P. Livi, F. L. Zawiślak, *Hyperfine Interactions* **5**, 219 (1978).

[7] H. Frauenfelder, R. M. Steffen, *Alpha-, Beta- and Gamma-Ray Spectroscopy* **2**, Ed. K.Siegbahn, North-Holland, Amsterdam 1965.
[8] E. N. Kaufmann, R. J. Vianden, *Rev. Mod. Phys.* **51**, 161 (1979).
[9] R. S. Raghavan, P. Raghavan, J. M. Friedt, *Phys. Rev. Lett.* **30**, 10 (1973).
[10] M. Minier, S. Ho Dung, *J. Phys. F* **7**, 503 (1977).
[11] A. C. Damask, G. J. Dienes, *Point Defects in Metals*, Gordon and Breach, New York 1963.
[12] W. B. Pearson, *Lattice Spacings and Structures of Metals and Alloys*, Pergamon, New York 1958.